UNIVERSITY OF AMSTERDAM

UvA-DARE (Digital Academic Repository)

A comparison of how deep brain stimulation in two targets with anti-compulsive efficacy modulates brain activity using fMRI in awake rats

Derksen, Maik; Zuidinga, Birte; van der Veer, Marijke; Rhemrev, Valerie; Jolink, Linda; Reneman, Liesbeth; Nederveen, Aart; Forstmann, Birte; Feenstra, Matthijs; Willuhn, Ingo; Denys, Damiaan

DOI
10.1016/j.pscychresns.2023.111611

Publication date
2023

Document Version
Final published version

Published in
Psychiatry Research - Neuroimaging

License
CC BY-NC-ND

Link to publication

Citation for published version (APA):
Derksen, M., Zuidinga, B., van der Veer, M., Rhemrev, V., Jolink, L., Reneman, L., Nederveen, A., Forstmann, B., Feenstra, M., Willuhn, I., & Denys, D. (2023). A comparison of how deep brain stimulation in two targets with anti-compulsive efficacy modulates brain activity using fMRI in awake rats. *Psychiatry Research - Neuroimaging*, *330*, Article 111611. https://doi.org/10.1016/j.pscychresns.2023.111611

General rights
It is not permitted to download or to forward/distribute the text or part of it without the consent of the author(s) and/or copyright holder(s), other than for strictly personal, individual use, unless the work is under an open content license (like Creative Commons).

Disclaimer/Complaints regulations
If you believe that digital publication of certain material infringes any of your rights or (privacy) interests, please let the Library know, stating your reasons. In case of a legitimate complaint, the Library will make the material inaccessible and/or remove it from the website. Please Ask the Library: https://uba.uva.nl/en/contact, or a letter to: Library of the University of Amsterdam, Secretariat, P.O. Box 19185, 1000 GD Amsterdam, The Netherlands. You will be contacted as soon as possible.

UvA-DARE is a service provided by the library of the University of Amsterdam (https://dare.uva.nl)

Download date:09 Nov 2026

Psychiatry Research: Neuroimaging 330 (2023) 111611

Contents lists available at ScienceDirect

Psychiatry Research: Neuroimaging

journal homepage: www.elsevier.com/locate/psychresns

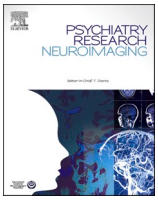

A comparison of how deep brain stimulation in two targets with anti-compulsive efficacy modulates brain activity using fMRI in awake rats

Maik Derksen [a,b], Birte Zuidinga [a], Marijke van der Veer [a], Valerie Rhemrev [a], Linda Jolink [a], Liesbeth Reneman [c], Aart Nederveen [c], Birte Forstmann [d], Matthijs Feenstra [a,b,†], Ingo Willuhn [a,b,†,*], Damiaan Denys [a,b,†]

[a] The Netherlands Institute for Neuroscience, Royal Netherlands Academy of Arts and Sciences, Amsterdam, The Netherlands
[b] Department of Psychiatry, Amsterdam University Medical Centers (location AMC), University of Amsterdam, Amsterdam, The Netherlands
[c] Department of Radiology and Nuclear Medicine, Amsterdam University Medical Centers (location AMC), University of Amsterdam, Amsterdam, The Netherlands
[d] University of Amsterdam, Integrative Model-based Cognitive Neuroscience Research Unit, Amsterdam, The Netherlands

ARTICLE INFO

Keywords:
Rodent fMRI
Human MRI scanner
Deep brain stimulation
VMS and IC stimulation
Neuromodulatory effects
Translational research

ABSTRACT

Deep brain stimulation (DBS) is an established neuromodulatory intervention against otherwise treatment-refractory obsessive-compulsive disorder (OCD). Several DBS targets, all of which are part of brain networks connecting basal ganglia and prefrontal cortex, alleviate OCD symptoms. Stimulation of these targets is thought to unfold its therapeutic effect by modulation of network activity through internal capsule (IC) connections. Research into DBS-induced network changes and the nature of IC-related effects of DBS in OCD is needed to further improve DBS.

Here, we studied the effects of DBS at the ventral medial striatum (VMS) and IC on blood-oxygen level dependent (BOLD) responses in awake rats using functional magnetic resonance imaging (fMRI). BOLD-signal intensity was measured in five regions of interest (ROIs): medial and orbital prefrontal cortex, nucleus accumbens (NAc), IC area, and mediodorsal thalamus. In previous rodent studies, stimulation at both target locations resulted in a reduction of OCD-like behavior and activation of prefrontal cortical areas. Therefore, we hypothesized that stimulation at both targets would result in partially overlapping BOLD responses.

Both differential and overlapping activity between VMS and IC stimulation was found. Stimulating the caudal part of the IC resulted in activation around the electrode, while stimulating the rostral part of the IC resulted in increased cross-correlations between the IC area, orbitofrontal cortex, and NAc. Stimulation of the dorsal part of the VMS resulted in increased activity in the IC area, suggesting this area is activated during both VMS and IC stimulation. This activation is also indicative of VMS-DBS impacting corticofugal fibers running through the medial caudate into the anterior IC, and both VMS and IC DBS might act on these fibers to induce OCD-reducing effects. These results show that rodent fMRI with simultaneous electrode stimulation is a promising approach to study the neural mechanisms of DBS. Comparing the effects of DBS in different target areas has the potential to improve our understanding of the neuromodulatory changes that take place across various networks and connections in the brain. Performing this research in animal disease models will lead to translational insights in the mechanisms underlying DBS, and can aid improvement and optimization of DBS in patient populations.

1. Introduction

Deep brain stimulation (DBS) is now an established neuromodulatory intervention for therapy-refractive obsessive compulsive disorder (OCD) (Graat et al., 2021; Hageman et al., 2021). It is generally thought that stimulation alters the activity across certain neural networks (Karas et al., 2019; Li et al., 2020; Balderman et al., 2021). At least four targets that are part of networks connecting the basal ganglia and (frontal) cortices have been used successfully, and stimulation at all these targets is affecting network activity of connections that are part of the internal capsule (IC) (Haber et al., 2021). Further research is needed to elucidate the nature of the IC-related effects of DBS in OCD in more

* Corresponding author.
† Authors contributed equally.

https://doi.org/10.1016/j.pscychresns.2023.111611
Received 13 May 2022; Received in revised form 21 December 2022; Accepted 6 February 2023
Available online 9 February 2023
0925-4927/© 2023 The Author(s). Published by Elsevier B.V. This is an open access article under the CC BY-NC-ND license (http://creativecommons.org/licenses/by-nc-nd/4.0/).

detail and to find out if other stimulation targets or paradigms can be found where stimulation may improve the 50–60% efficacy that has been reported up to now (van Westen et al., 2021).

Animal research may be used to probe these circuits experimentally (Haber et al., 2021; Feenstra & Denys, 2012; Klanker et al., 2017). We recently proposed to use functional magnetic resonance imaging (fMRI) in awake rats to describe DBS effects across forebrain networks (Derksen et al., 2021). Stimulation sites were defined in rats (van Dijk et al., 2013) and validated in Sapap3 mutant mice (Pinhal et al., 2018) which is an animal model for OCD (Welch et al., 2007). Stimulation of the IC and, to a lesser extent, the ventromedial striatum (VMS), was very effective in reducing compulsive self-grooming in these mice (Pinhal et al., 2018). As a first possible indication of underlying network effects, it was found that stimulation of both targets induced c-Fos expression in medial prefrontal cortical areas, indicative of neuronal activation in these prefrontal areas.

Here, we studied the effects of DBS at IC and VMS on BOLD responses in awake rats. We hypothesized that stimulation of these two targets would lead to partially overlapping effects, reflecting the behavioral efficacy of using these targets in the OCD mouse model. Therefore, we studied BOLD responses throughout the forebrain and focused on activation of five ROIs: medial and orbital prefrontal cortex, nucleus accumbens, IC, and mediodorsal thalamus.

2. Methods

The Methods are based on those described in Derksen et al. (2021), except when indicated below.

2.1. Subjects

Forty-five (45) adult male Wistar rats (250–350 g, Charles River Laboratories, Saint-Germain-sur-l'Arbreste, France) were included in this study. After excluding animals due to off-target electrode placements or images containing MR artifacts ($n = 12$), 16 animals remained in the VMS targeted group and 17 in the IC targeted group. Our findings are limited to males as no female rats were included in this study. However, we have no reason to assume that this influenced the outcome of the experiments performed.

All animals were individually housed with ad-libitum access to food and water, on a normal day-night cycle (lights on 7am to 7pm). The experiments were approved by the Animal Experimentation Committee of the Royal Netherlands Academy of Arts and Sciences (KNAW) and carried out in agreement with Dutch law (Wet op de Dierproeven, 1996) and European regulations (Guideline 2010/63/EU).

2.2. Stimulation electrodes

The stimulation electrodes were composed of two intertwined silver wires (99% pure silver, Advent Research Materials Ltd, Oxford, UK) with a bare wire diameter of 0.125 mm and a 26 μm PTFE coating. At the tips, approximately 200 μm of the coating was stripped, and the tips themselves were spaced 250 μm apart. Each lead end of the electrode was connected to a 7 mm-long sterling silver tube (outer/inner diameter 1.5/1.0 mm, Bijou Moderne Bleiswijk, the Netherlands). The sterling silver tubes were kept in place by a plastic holder, serving as a connector for the stimulation cables. For a more detailed description of the electrode fabrication, see Derksen et al., 2021.

2.3. Stereotaxic surgery

Surgery, for the purpose of implanting the stimulation electrodes and attaching a plastic pedestal to the skull, was performed after a minimum of one week of acclimatization. The animals were put under isoflurane anesthetics (3% induction, 1.8–2.5% maintenance, 1:1 air in oxygen at 0.3 L/min, Isoflo, Zoetis, Rotterdam, the Netherlands). Temperature was kept at 37 °Celsius by means of a heating pad. After a sagittal incision, the skull was exposed. Two burr holes were drilled, allowing for bilateral DBS electrode implants, targeting either the VMS (AP + 1.72 mm, ML +/- 1.60 mm, DV–6.8 mm from bregma) or the IC (AP – 0.8 mm, ML +/- 2.1 mm, DV −6.8 mm from bregma) (Paxinos and Watson, 2007). Please note that the VMS target was previously called (ventromedial) caudate (van Dijk et al., 2013) and dorsal part of the ventral striatum (Pinhal et al., 2018). Two plastic screws, placed rostrally to the electrodes, were used to secure the electrodes, together with dental cement (Simplex Rapid, Kemdent, Swindon, UK). Caudally to the electrodes, a plastic head pedestal (used to fixate the animal's head in the MRI-setup) was attached to the animal's skull by means of three plastic screws and dental cement. Then, the wound was closed with sutures and the animals were given a post-op meloxicam injection (1 mg/kg, Metacam, Boehringer Ingelheim Vetmedica Ltd., Duluth, GA, US). The animals had a recovery time of one-week minimum before taking part in the experiment. For a more detailed description and images of the custom-made MRI rat restrainer, the electrodes and head pedestal, see Derksen et al., 2021.

2.4. fMRI preparation

The animals were shortly put under isoflurane (3%, 1:1 air in oxygen at 0.3 L/min) in order to place them in the custom-made MRI rat restrainer (Derksen et al., 2021). The animal's top incisors were put over a bite-bar, and its head was fixated into the setup by screwing the head pedestal tightly into a holder, part of the restrainer setup. The animal's body was placed into a clear plastic tube, constricting body movement. A pneumatic pillow was placed underneath the animal's body for monitoring respiration (Small Animal Instruments, Inc., Stony Brook, New York, United States). A custom-made, two-channel receiver coil (MRCoils, Zaltbommel, the Netherlands) was placed over the animal's head, after which the whole setup was placed inside a 3T clinical scanner (Philips Healthcare, Best, the Netherlands). The DBS electrodes were connected with carbon wires to a digital stimulator located outside of the scanner room (DS8000, World Precision Instruments, Berlin, Germany) through stimulus isolators. These digital linear stimulus isolators (DSL1000, WPI, Berlin, Germany), located outside of the scanner room and connected to the patch bay, were used to deliver constant current from the stimulator to the electrodes. Ferrite chokes were placed around the cables leading from the stimulus isolators to the patch bay, as to suppress high frequency interference. For a more detailed description and images of the custom-made MRI rat restrainer, the custom-made receiver coil and the placement of the setup in the clinical scanner, see Derksen et al., 2021.

2.5. fMRI acquisition and deep brain stimulation (DBS)

The methods as described by Derksen et al. (2021) included a week of repeated training sessions to accustom the animals to the restrainer and scanner noise. As measures of stress and movements were not altered by these training sessions, they were omitted in the present procedures.

MR images were acquired on a 3.0T Philips Ingenia MR system (Philips Healthcare, Best, the Netherlands). During the scout scans, the animals were kept under a maintenance dose of isoflurane (1.8 – 2.0%, in medical air at 0.6 L/min) to prevent possible motion artifacts. Then, anesthetics were discontinued, and functional MR imaging (fMRI) was started when the respiration rate of the animal reached 100 breaths per minute. fMRI images were obtained by multi-shot spin-echo (SE) echo planar imaging (EPI) with interleaved slice acquisition and no slice gap (EPI factor = 9, TR = 1000 ms, TE = 45 ms, dynamic acquisition time = 5000 ms, voxel size = 0.55 × 0.55 × 1.5 mm, matrix size = 64 × 57, 12 slices).

During this EPI sequence, DBS (a biphasic, constant current, 80 μs pulse width at 130 Hz, 300 μA stimulation) was delivered to the animals.

The stimulation protocol consisted 20 s of DBS (which equals 4 vol), followed by 40 s of no stimulation (8 vol), which was repeated 10 times. Preceding these 10 repetitions, 8 dummy scans and 40 s of baseline recordings were obtained. In total, the animals were unanesthetized for 11 min and 20 s during the EPI sequence acquisition: 40 s during the dummy scans, 40 s during baseline recording, and 10 min during the stimulation protocol.

After collecting the functional MR data, the animals were again anesthetized with isoflurane (3%, 1:1 air in oxygen at 0.3 L/min) and a T2-weighted anatomical image was obtained using a multi-shot turbo spin echo (TSE) sequence (TSE factor = 8, TR = 4000 ms, TE = 56 ms, voxel size = 0.2 × 0.2 × 1.5 mm, matrix size = 176 × 168, 12 slices, interleaved slice acquisition, no slice gap). The total scan duration for the anesthetized T2-weighted anatomical image was 2 min and 56 s. The animals were then removed from the scanner and restrainer device. While still under anesthetics, the DBS electrodes were connected to a stimulus generator (WPI A365, World Precision Instruments, Berlin, Germany) and electrical lesions were made (500 μA direct current for 20 s) for determining electrode tip locations. The animals were then euthanized by terminal cardiac puncture after which the brains were removed, flash frozen and stored at -80 degrees Celsius for histological investigation at a later time.

2.6. Data processing and analyses

2.6.1. Brain extraction and study-specific, standard-space anatomical and functional templates

The raw anatomical and EPI data were converted from DICOM to NifTI format using the MRIcron/dcm2nii tool (Chris Rorden, 4AUGUST2017 (Debain) 64-bit BSD License). Voxel sizes were modified to ten times their original sizes using ImageJ (version 1.50d, National Institutes of Health, Bethesda, Maryland, USA), to better accommodate the preprocessing algorithms of the FMRIB Software Library (FSL, Analysis Group, FMRIB, Oxford UK). Motion correction of the fMRI time series was carried out using the Motion Correction tool of the FMRIB's Linear Image Registration Tool (MCFLIRT), using a 6 degrees of freedom (DOF) transformation and a hand-picked reference volume in the middle of the time series. All anatomical and BOLD images had the brain segment extracted using the FMRIB's Brain Extraction Tool (FLS/BET). Anatomical and BOLD templates were produced by registering the individual brain-extracted images to one representative image, anatomical or BOLD respectively, and taking the median of those images. This procedure was then repeated, this time using the previously created median image as target for registration. Registrations were performed using a combination of linear and non-linear registration (using FMRIB's Linear Image Registration Tool (FLIRT) and FMRIB's Nonlinear Image Registration Tool (FNIRT), respectively) and carefully inspected visually. Templates were created for the VMS targeted and IC targeted groups separately.

2.6.2. ROI-based signal intensity analysis

- ROI selection

A number of ROIs, associated with the CSTC circuit, were selected for use in ROI-based signal intensity analyses, namely the orbitofrontal cortex (OFC), medial prefrontal cortex (mPFC, consisting of the infralimbic and prelimbic cortex), the mediodorsal thalamus (mdThal) and the area around the electrode tip (either in the VMS or IC for the VMS-stimulated and IC-stimulated groups respectively) (Fig. 1). For each animal, a separate set of ROIs was created to fit their BOLD time series.

ROIs for the region around the electrode tips consisted of rectangles sized 5 × 7 voxels for each tip, hand drawn in the slice containing the electrode in the coronal plane. This was done for each animal individually. The electrode tip was located in the middle of the rectangle, and the electrode tract itself was removed from the ROI (approximately 12 voxels per rectangle). For the area around the electrode tip in the IC-stimulated group, this results in a ROI that exceeds the boundaries of the internal capsule and partially encompasses the globus pallidus (GP) and reticular thalamic nucleus (RT) as well. Reducing the ROI size would have resulted in too few voxels for the analysis, and would have hampered the comparability with the ROI around the electrode in the VMS-stimulated group. For the same reason of comparability, the analogous ROI in the VMS-stimulated group was chosen to encompass a part of GP and RT as well as the IC.

The other ROIs were extracted from an MRI rat brain atlas (Schwarz et al., 2006). This MRI rat brain atlas was registered to the study specific anatomical template. The resulting registration matrix was applied to the ROIs extracted from the MRI rat brain atlas, fitting them to the study specific anatomical template. Next, each individual BOLD time series was registered to the corresponding anatomical image, and each anatomical image was registered to the study specific templates. The resulting two transformation matrices were then inversely applied to the ROIs, transforming them to the individual functional space of each animal. Registrations were performed using a combination of linear and non-linear registration, using FMRIB's FLIRT and FNIRT, and carefully inspected visually in the coronal plane, anterior to posterior. The transformations were done using the VMS and IC study specific

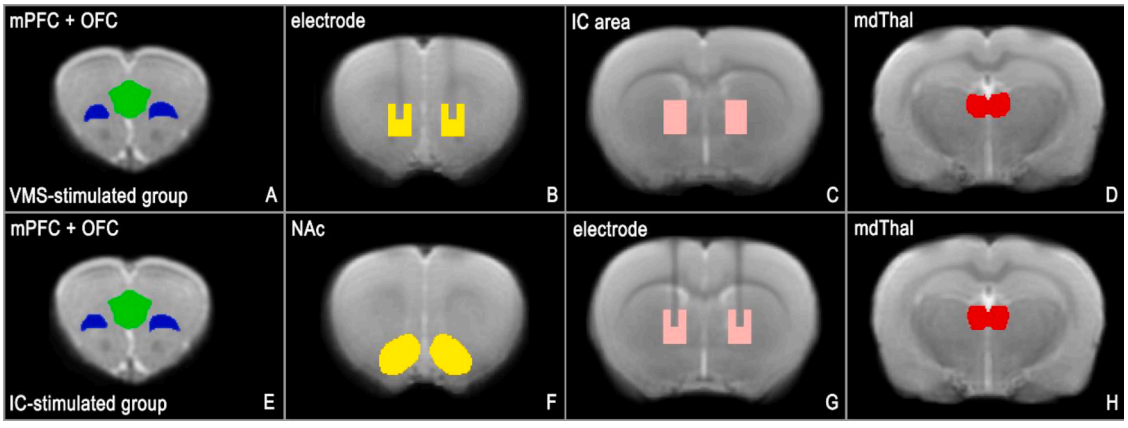

Fig. 1. Overview of selected ROIs for use in ROI-based signal intensity analyses. The top row shows the ROIs selected for use within the VMS-stimulated group in the coronal plane (A: medial prefrontal cortex (mPFC) and orbital frontal cortex (OFC); B: area around the electrode; C: internal capsule area (ICarea); D: medial dorsal thalamus (mdThal)), the bottom row shows the ROIs selected for use within the IC-stimulated group (E: mPFC and OFC; F: nucleus accumbens (NAc); G: area around the electrode; H: mdThal). The ROIs in these images are projected on study-specific functional MRI template images - in the study itself, the ROIs are registered to each individual animal for extraction of the time-series.

templates for the corresponding groups.

○ ROI-based signal intensity analyses

For each ROI described previously, the time-series was extracted as an average of all voxels within the ROI. Time-series were extracted from the motion-corrected functional data. Then, the time-series were cut up in time-points recorded during the ON periods (4 vol) and time-points recorded during the last 4 vol of the OFF periods. These were then averaged as signal intensity during DBS-ON and signal intensity during DBS-OFF, per stimulation-group, per ROI, and per individual animal.

In order to analyze the differences between the average signal intensities measured during the DBS-ON periods against those measured during the DBS-OFF periods in a specified ROI, a Bayesian paired *t*-test framework available in JASP (JASP Team, 2021, version 0.15.0.0) was used. Assumptions of normality were checked by visually investigating Q-Q plots and performing the Shapiro-Wilk test. All null hypotheses postulate that there are no differences between signal intensities measured during DBS-ON and DBS-OFF, setting the effect sizes δ for H_0 at zero. The alternative hypotheses, that stimulation of a target location induces changes in the specified ROIs, were one-tailed, with an effect size δ for $H_1 >$ zero, assuming that the effect of DBS-ON on signal intensity is greater than DBS-OFF. As we had no informed effect size expectations, all t-tests were performed with the default Cauchy prior scaling factor sqrt(2)/2. For each of the one-sided paired t-tests, the Bayes factor robustness check was performed over a wide range of Cauchy prior widths. The histological examination of the electrode locations (see: Results – Electrode location) showed that it is possible to group animals into sub-location targeted groups: caudate nucleus (NCaud) and nucleus accumbens (NAc) stimulated animals within the VMS-group, and rostrally and caudally stimulated animals within the IC-group. The analyses described here are therefore performed for the VMS and IC targeted groups in general, and the sub-location targeted groups.

○ Cross-correlation analyses

For investigating cross-correlations, the extracted time series were cut up in time-points recorded during the ON periods (4 vol) and time-points recorded during the last 4 vol of the OFF periods. All time-points during DBS-ON were then put together in sequence, as were the time-points during the DBS-OFF periods, resulting in a time-course of only DBS-ON time-points and one with only DBS-OFF time-points. Cross-correlations coefficients were calculated for the cross-correlations between 'the area around the electrode' and the other four specified ROIs (for the VMS-stimulated group: mPFC, OFC, IC area, and medial dorsal thalamus; for the IC-stimulated group: mPFC, OFC, NAc, and medial dorsal thalamus), for the DBS-ON and DBS-OFF periods, using the Matlab (The MathWorks Inc, version 8.5.0 (R2015a), Natick, Massachusetts) correlation coefficient function.

The Bayesian paired *t*-test framework available in JASP was used to assess differences in cross-correlation coefficients between DBS-ON and DBS-OFF periods. Paired t-tests were then performed for each of the four combinations of 'area around the electrode' and the other four specified ROIs, using the cross-correlation coefficients calculated for those combinations. Assumptions of normality were checked by visually investigating Q-Q plots and performing the Shapiro-Wilk test. All null hypotheses postulate that there are no differences between the cross-correlation coefficients calculated from the DBS-ON and DBS-OFF periods, setting the effect sizes δ for H_0 at zero. The alternative hypotheses were one-tailed, with an effect size δ for $H_1 >$ zero, assuming that the effect of DBS-ON on the cross-correlation is greater than DBS-OFF. As we had no informed effect size expectations, all t-tests were performed with the default Cauchy prior scaling factor sqrt(2)/2. For each of the one-sided paired t-tests, the Bayes factor robustness check was performed. The histological examination of the electrode locations (see: Results – Electrode location) showed that it is possible to group animals into sub-location targeted groups: NCaud and NAc stimulated animals within the VMS-group, and rostrally and caudally stimulated animals within the IC-group. The analyses described here are therefore performed for the VMS and IC targeted groups in general, and the sub-location targeted groups.

All analyses mentioned here were performed as Bayesian analyses. For interpretation of the Bayes factors BF_{10} and BF_{01}, please refer to Table 1 which shows the labels used in this publication, as proposed by Jeffreys (1961) and adjusted by van Doorn et al. (2021).

3. Results

3.1. Electrode placement

Electrode placement was determined by histological examination in the entire group of IC-stimulated animals. For 8 of the 16 animals in the VMS-stimulated group, no histological data was available and electrode placement was determined using the anatomical MRI scans. A spread in electrode positions was observed, such that half of the VMS-targeted electrodes were located in the nucleus accumbens and the other half in the caudate nucleus. The IC-targeted electrodes were distributed over the AP-axis and could be separated in rostral and caudal subgroups. In the VMS-stimulated group, all animals with both the electrode tips targeting the NCaud were placed in the NCaud-stimulated sub-location group, and animals with both electrode tips targeting the NAc were placed in the NAc-stimulated sub-location group. One animal had one electrode tip targeted at the NCaud and the other at the NAc, and was therefore excluded. This resulted in groups of 8 animals with NCaud-stimulation and 7 animals with NAc-stimulation. In the IC-stimulated group, a subdivision of animals with electrodes targeting the rostral part of the IC and the caudal part of the IC was made. Electrode locations within the IC-stimulated group ranged from -0.48 mm to -1.80 mm distance from bregma (Paxinos and Watson, 2007). Animals with both electrode tips within the -0.48 mm to -1.12 mm from bregma range were included in the rostral IC-stimulated group, and those with both tips within the -1.16 mm to -1.80 mm from bregma range were included in the caudal IC-stimulated group. One animal did not have both electrode tips in either rostral or caudal IC and was therefore exclude. This resulted in groups of 8 animals with rostral IC-stimulation, and 7 animals with caudal IC-stimulation. An overview of the electrode locations can be found in Fig. 2.

3.2. ROI analyses

3.2.1. VMS

In order to analyze the differences between the average signal intensities measured during the DBS-ON periods against those measured during the DBS-OFF periods in a specified ROI, the Bayesian paired *t*-test framework available in JASP was used. Paired t-tests were performed for each ROI, firstly for all of the animals included in the VMS-stimulated group, and secondly for the animals included in the NCaud- and NAc-stimulated sub-location groups separately. An overview of the t-test

Table 1
Interpretation of BF_{10} and BF_{01}. Suggested categories for interpreting the Bayes factors. Adapted from van Doorn et al., 2021.

Interpretation of Bayes factors			
Bayes factor BF_{10}			Interpretation
	>	30	Very strong evidence for H1
10	–	30	Strong evidence for H1
3	–	10	Moderate evidence for H1
0	–	3	Weak evidence for H1
Bayes factor BF_{01}			**Interpretation**
0	–	3	Weak evidence for H0
3	–	10	Moderate evidence for H0
10	–	30	Strong evidence for H0
	>	30	Very strong evidence for H0

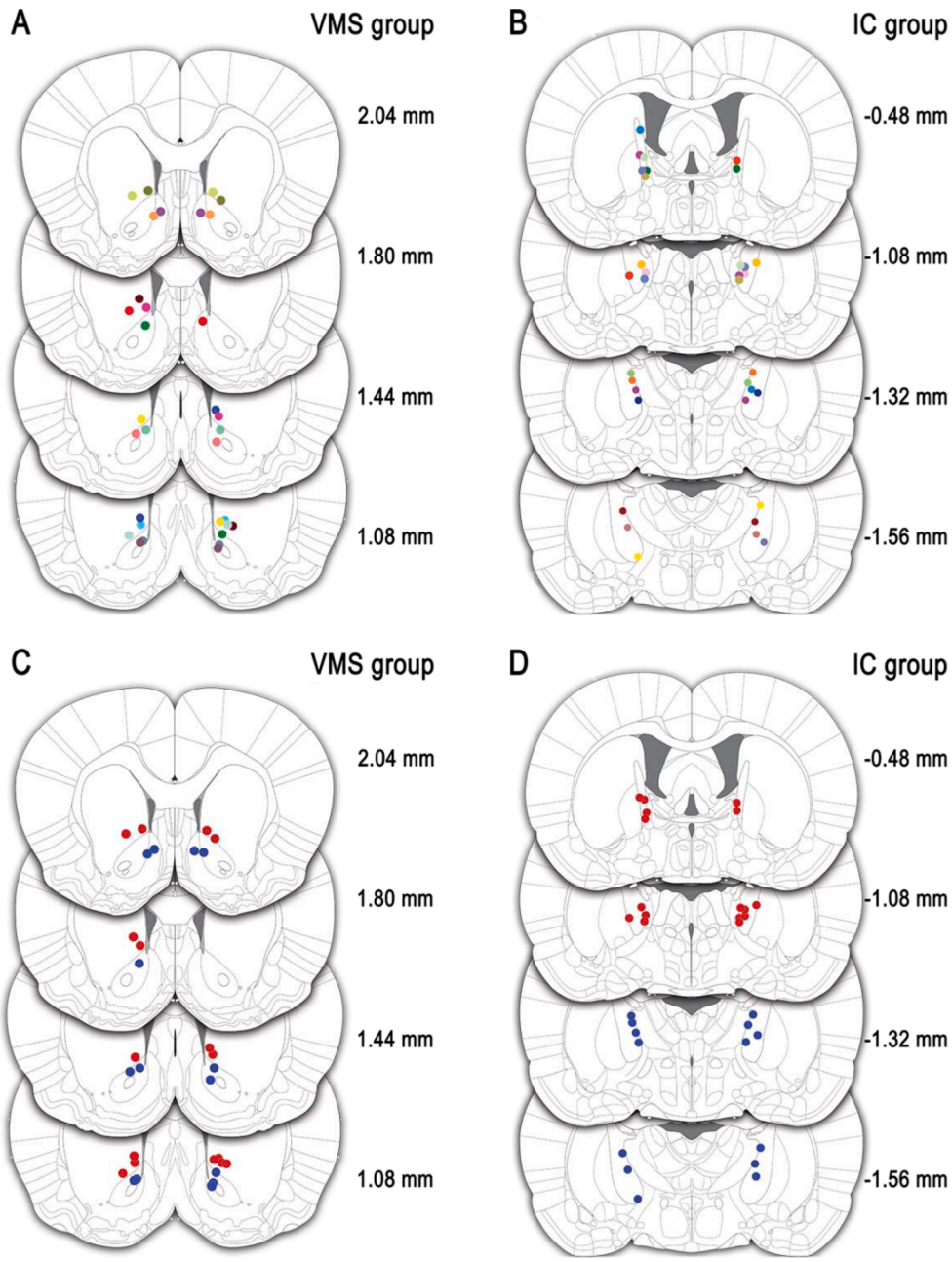

Fig. 2. Overview of electrode-tip locations determined by histology and MRI. Colored dots superimposed on coronal slices (adapted from Paxinos and Watson, 2007), indicating the location of the DBS-electrode tips in the ventral-medial striatum (VMS) (A, $n = 16$) and the internal capsule (IC) (B, $n = 17$) stimulated groups, with a unique color for each animal and identical colors representing the locations in the left and right hemisphere of the bilateral implants. Also shown is the division of sub-locations of the electrode tips within the VMS-stimulated group (C), with red dots indicating the nucleus caudatus (NCaud) as sub-location ($n = 8$) and blue dots indicating the nucleus accumbens (NAc) as sub-location ($n = 7$), and the sub-locations within the IC-stimulated group (D), with red dots indication the rostral IC as sub-location ($n = 8$) and blue dots indicating the caudal IC as sub-location ($n = 7$). Numbers indicate distance from bregma.

results can be found in Table 2.

There is moderate evidence supporting the hypothesis that stimulating the VMS induces higher signal intensities in the IC area during DBS-ON periods ($M = 10{,}557$, SE = 114.0) compared to DBS-OFF ($M = 10{,}529$, SE = 139.9), with the data being around 3 times more likely to occur under this hypothesis than under the null hypothesis ($BF_{10} = 3.045$, error% < 0.001). The robustness check for this Bayes factor shows a Bayes factor range from 2.1 to 3.4 over a wide range of prior widths. For the remaining ROIs (mPFC, OFC, medial dorsal thalamus, and the area around the electrode) there is moderate evidence supporting the null hypothesis. It is around 3 to 6 times more likely for the data to occur under the null hypothesis in these ROIs than under the alternative hypothesis (mPFC: $BF_{01} = 3.353$, error% < 0.005; OFC: $BF_{01} = 6.471$, error% < 0.001; medial dorsal thalamus: $BF_{01} = 4.533$, error% < 0.005; area around the electrode: $BF_{01} = 5.811$, error% < 0.001).

The data from stimulating the NCaud shows strong support for the hypothesis that stimulating this sub-location of the VMS induces higher signal intensities in the IC area during the DBS-ON period ($M = 10{,}660$, SE = 194.9) compared to DBS-OFF period ($M = 10{,}607$, SE = 187.3), with the data being around 16 times more likely to occur under this hypothesis than under the null hypothesis ($BF_{10} = 16.21$, error% < 0.001). The robustness check for this Bayes factor shows a Bayes factor range of 16.2 to 17.2 over a wide range of prior widths. The data from the OFC and medial thalamus both are about 3 times more likely to occur under the null hypothesis, than under the alternative hypothesis, providing moderate support for the null hypothesis in these ROIs (OFC: $BF_{01} = 3.213$, error% < 0.001; medial dorsal thalamus: $BF_{01} = 3.584$, error% < 0.005). For the remaining ROIs (mPFC and area around the electrode) only weak evidence was found for both BF_{10} and BF_{01}.

When looking at the data from the NAc-stimulated group, only weak evidence for the hypothesis that stimulating this area induces higher signal intensities in the specified ROIs during DBS-ON compared to DBS-OFF was found. For the mPFC, OFC, medial dorsal thalamus, and the area around the electrode, the data from those ROIs is around 4 to 5

Table 2
Results from the ROI analyses in the VMS-stimulated group. Shown here are the average signal intensities (mean ± SEM) during DBS-ON and DBS-OFF and the Bayes factors (BF_{10} and BF_{01}) resulting from the paired *t*-test framework comparing those averages, assuming the one-tailed alternative hypothesis that DBS-ON results in higher signal intensities compared to DBS-OFF. The results are shown for the VMS as DBS target location (VMS –all, $n = 16$) and the sub-locations within the VMS (caudate nucleus (VMS –NCaud), $n = 8$; nucleus accumbens (VMS –NAc), $n = 7$). For each target location, t-tests were performed for five ROIs (mPFC = medial prefrontal cortex; OFC = orbitofrontal cortex; electrode = area around the electrode tip; IC area; mdThal = medial dorsal thalamus). Bayes factors displayed in bold indicate moderate or greater evidence found.

Stimulation location	ROI	DBS-ON	DBS-OFF	BF_{10}	BF_{01}
VMS -all $n = 16$	mPFC	11,626 ± 322.1	11,620 ± 316.1	0.298	**3.353**
	OFC	11,589 ± 249.5	11,600 ± 246.3	0.155	**6.471**
	electrode	10,372 ± 232.5	10,382 ± 237.5	0.172	**5.811**
	IC area	10,557 ± 144.0	10,529 ± 139.9	**3.045**	0.382
	mdThal	10,264 ± 92.76	10,269 ± 88.66	0.221	**4.533**
VMS -NCaud $n = 8$	mPFC	12,127 ± 541.8	12,104 ± 529.2	0.956	1.046
	OFC	11,853 ± 427.9	11,855 ± 421.1	0.311	**3.213**
	electrode	10,730 ± 383.9	10,725 ± 400.3	0.384	2.601
	IC area	10,660 ± 194.9	10,607 ± 187.3	**16.21**	0.062
	mdThal	10,290 ± 108.0	10,297 ± 97.1	0.279	**3.584**
VMS –NAc $n = 7$	mPFC	11,119 ± 325.2	11,133 ± 329.6	0.259	**3.855**
	OFC	11,319 ± 291.7	11,340 ± 291.8	0.210	**4.760**
	electrode	10,058 ± 246.5	10,086 ± 246.5	0.194	**5.147**
	IC area	10,548 ± 227.5	10,540 ± 227.9	0.471	2.121
	mdThal	10,179 ± 169.8	10,205 ± 162.7	0.204	**4.902**

Table 3
Results from the ROI analyses in the IC-stimulated group. Shown here are the average signal intensities (mean ± SEM) during DBS-ON and DBS-OFF and the Bayes factors (BF_{10} and BF_{01}) resulting from the paired t-test framework comparing those averages, assuming the one-tailed alternative hypothesis that DBS-ON results in higher signal intensities compared to DBS-OFF. The results are shown for the internal capsule (IC) as DBS target location (IC –all, $n = 17$) and the sub-locations within the IC (IC –rostral, $n = 8$; IC -caudal, $n = 7$). For each target location, t-tests were performed for five ROIs (mPFC = medial prefrontal cortex; OFC = orbitofrontal cortex; NAc = nucleus accumbens; electrode = area around the electrode tip – including internal capsule and parts of globus pallidus and reticular thalamic nucleus; mdThal = medial dorsal thalamus). Bayes factors displayed in bold indicate moderate or greater evidence found.

Stimulation location	ROI	ON	OFF	BF_{10}	BF_{01}
IC –all $n = 17$	mPFC	10,953 ± 156.6	11,080 ± 177.0	0.145	**6.886**
	OFC	10,963 ± 156.5	10,930 ± 158.7	1.902	0.562
	NAc	10,144 ± 183.0	10,032 ± 162.6	1.341	0.746
	electrode	10,137 ± 104.0	10,110 ± 99.7	**4.129**	0.242
	mdThal	10,256 ± 82.14	10,256 ± 88.46	0.252	**3.976**
IC -rostral $n = 8$	mPFC	10,906 ± 220.8	10,913 ± 217.7	0.281	**3.565**
	OFC	10,576 ± 162.6	10,743 ± 164.8	0.516	1.937
	NAc	9999 ± 177.8	10,009 ± 163.8	0.261	**3.835**
	electrode	10,014 ± 159.6	10,004 ± 160.3	0.620	1.613
	mdThal	10,275 ± 138.1	10,263 ± 148.1	0.615	1.625
IC –caudal $n = 7$	mPFC	11,030 ± 258.4	10,994 ± 258.4	0.760	1.320
	OFC	10,925 ± 254.6	10,876 ± 269.6	1.383	0.723
	NAc	10,285 ± 299.9	10,023 ± 250.8	1.714	0.583
	electrode	10,278 ± 151.1	10,238 ± 143.3	**4.669**	0.214
	mdThal	10,345 ± 96.64	10,359 ± 111.1	0.272	**3.672**

times more likely to occur under the null hypothesis than under the alternative hypothesis (mPFC: $BF_{01} = 3.855$, error% < 0.01; OFC: $BF_{01} = 4.760$, error% < 0.001; medial dorsal thalamus: $BF_{01} = 4.902$, error% < 0.001; area around the electrode = 5.147, error% < 0.0001) providing moderate support for the null hypothesis in these ROIs.

In conclusion, these data indicate that the only ROI where VMS-DBS results in increased activity is the IC area and that the evidence for this is strong when the electrodes are exclusively positioned in the caudate part of the VMS.

3.2.2. IC

In order to analyze the differences between the average signal intensities measured during the DBS-ON periods against those measured during the DBS-OFF periods in a specified ROI, the Bayesian paired *t*-test framework available in JASP was used. Paired t-tests were performed for each ROI, firstly for all of the animals included in the IC-stimulated group, and secondly for the animals included in the rostral- and caudal IC-stimulated sub-location groups separately. An overview of the t-test results can be found in Table 3.

There is moderate evidence supporting the hypothesis that stimulating the IC induces higher signal intensities in the area around the electrode during DBS-ON periods ($M = 10{,}137$, SE = 104,0) compared to DBS-OFF ($M = 10{,}110$, SE = 99.7), with the data around 4 times more likely to occur under this hypothesis than under the null hypothesis ($BF_{10} = 4.129$, error% < 0.005). Note that the area around the electrode encompasses not only the internal capsule but also parts of globus pallidus and the reticular thalamic nucleus. As a robustness measure of the Bayes factor, the Bayes factor ranges from 2.9 to 4.5 over a range of prior widths. For the mPFC and medial dorsal thalamus there is moderate evidence supporting the null hypothesis, with the data around 4 to 6 times more likely to occur under the null hypothesis in these ROIs than under the alternative hypothesis (mPFC: $BF_{01} = 6.886$, error% < 0.0001; medial dorsal thalamus: $BF_{01} = 3.976$, error% < 0.005). For the OFC and NAc, there is only weak evidence supporting either the alternative or null hypothesis.

When looking at the data from the rostral IC-stimulated group, only weak evidence for the hypothesis that stimulating this area induces higher signal intensities in the specified ROIs during DBS-ON compared to DBS-OFF was found. For the mPFC and NAc, the data from those ROIs is around 3 to 4 times more likely to occur under the null hypothesis than under the alternative hypothesis (mPFC: $BF_{01} = 3.565$, error% < 0.005; NAc = 3.835, error% < 0.001) providing moderate support for the null hypothesis in these ROIs. For the other ROIs (OFC, area around the electrode, and medial dorsal thalamus), only weak evidence supporting the null hypothesis was found.

The data from stimulating the caudal part of the IC shows strong support for the hypothesis that stimulating this sub-location induces higher signal intensities in the area around the electrode during the DBS-ON period ($M = 10{,}278$, SE = 151.1) compared to DBS-OFF ($M = 10{,}238$, SE = 143.3), with the data around 5 times more likely to occur

under this hypothesis than under the null hypothesis (BF_{10} = 4.669, error% < 0.0001). Note that the area around the electrode encompasses the internal capsule and parts of the GP and RT. The robustness check for this Bayes factor shows a Bayes factor range of 4.1 to 4.7 over a wide range of prior widths. The data from the medial thalamus is around 3.5 times more likely to occur under the null hypothesis than under the alternative hypothesis, providing moderate support for the null hypothesis in this ROI (BF_{01} = 3.672, error% < 0.01). For the remaining ROIs (mPFC, OFC, and NAc) only weak evidence was found for both BF_{10} and BF_{01}.

Summarizing the results of IC DBS: the only ROI where stimulation results in increased activity is the area around the electrode. This effect is associated exclusively with a caudal placement of the electrodes.

3.3. Cross-correlation analyses

3.3.1. VMS

In order to analyze the differences between cross-correlations measured during the DBS-ON periods against those measured during the DBS-OFF periods, a Bayesian paired *t*-test framework available in JASP was used. Paired t-tests were performed for each of the four combinations of 'area around the electrode' and the other specified ROIs (mPFC, OFC, IC, and medial dorsal thalamus), using the cross-correlation coefficients calculated for those combinations. This was done firstly for all of the animals included in the VMS-stimulated group, and secondly for the animals included in the NCaud- and NAc-stimulated sub-location groups separately. An overview of the t-test results can be found in Table 4.

The cross-correlation coefficients found during the DBS-ON periods when stimulating the VMS, range from 0.143 to 0.292, which can be considered to be representing weak cross-correlations between the area around the electrode and the other four specified ROIs. During the DBS-OFF periods these coefficients all range from 0.025 to 0.163. When looking at the effect of VMS-stimulation on changes in cross-correlation between the area around the electrode and the other specified ROIs, there is only weak evidence supporting the alternative hypothesis that stimulation of the VMS results in stronger cross-correlations between the area around the electrode and other specified ROIs, and only weak evidence supporting the null hypothesis that the VMS stimulation has no effect on the cross-correlations found.

Similarly, when stimulating the VMS sub-locations NCaud or NAc, the cross-correlation coefficients found can be considered to indicate weak cross-correlations between the sub-locations and the other four specified ROIs, with coefficients ranging from 0.103 to 0.336 during DBS-ON, and 0.010 to 0.241 during the DBS-OFF periods. When looking at the effect of either NCaud or NAc stimulation on changes in cross-correlation between the sub-locations and the other specified ROIs, only weak evidence is found to support the alternative hypothesis, and only weak evidence is found to support the null hypothesis.

In summary, these analyses do not support any stimulation-related change in cross- correlation between the VMS area around the electrode and any of the ROIs.

Table 4
Results from the cross-correlation analyses in the VMS stimulated group. Shown here are the average cross-correlation coefficients (mean ± SEM) calculated during DBS-ON and DBS-OFF, and the Bayes factors (BF_{10} and BF_{01}) resulting from the paired *t*-test framework comparing those averages, assuming the one-tailed alternative hypothesis that DBS-ON results in higher cross-correlations compared to DBS-OFF. The results are shown for the VMS as DBS target location (VMS –all, n = 16) and the sub-locations within the VMS (caudate nucleus (VMS –NCaud), n = 8; nucleus accumbens (VMS –NAc), n = 7). For each target location, t-tests were performed on the cross-correlation coefficients found between the area around the electrode tip and the four other ROIs (electrode = area around the electrode tip; mPFC = medial prefrontal cortex; OFC = orbitofrontal cortex; IC area; mdThal = medial dorsal thalamus). No Bayes factors providing moderate or greater evidence were found.

Stimulation location	ROI	ON	OFF	BF_{10}	BF_{01}
VMS -all n = 16	electrode - mPFC	0.169 ± 0.071	0.094 ± 0.070	0.448	2.234
	electrode - OFC	0.143 ± 0.085	0.040 ± 0.083	0.544	1.839
	electrode – IC area	0.292 ± 0.053	0.163 ± 0.084	1.127	0.887
	electrode - mdThal	0.153 ± 0.063	0.025 ± 0.076	0.949	1.058
VMS -NCaud n = 8	electrode - mPFC	0.216 ± 0.097	0.130 ± 0.118	0.491	2.035
	electrode - OFC	0.103 ± 0.122	0.021 ± 0.145	0.483	2.071
	electrode – IC area	0.270 ± 0.091	0.241 ± 0.101	0.404	2.477
	electrode - mdThal	0.172 ± 0.083	0.082 ± 0.105	0.599	1.670
VMS -NAc n = 7	electrode - mPFC	0.115 ± 0.124	0.068 ± 0.243	0.429	2.332
	electrode - OFC	0.136 ± 0.134	0.062 ± 0.105	0.471	2.123
	electrode – IC area	0.336 ± 0.064	0.168 ± 0.123	1.109	0.901
	electrode - mdThal	0.122 ± 0.116	0.010 ± 0.121	0.623	1.606

3.3.2. IC

In order to analyze the differences between cross-correlations measured during the DBS-ON periods against those measured during the DBS-OFF periods, the Bayesian paired *t*-test framework available in JASP was used. Paired t-tests were performed for each of the four combinations of 'area around the electrode' and the other specified ROIs (mPFC, OFC, NAc, and medial dorsal thalamus), using the cross-correlation coefficients calculated for those combinations. This was done firstly for all of the animals included in the IC-stimulated group, and secondly for the animals included in the rostral IC- and caudal-stimulated sub-location groups separately. An overview of the t-test results can be found in Table 5.

The cross-correlation coefficients found during DBS-ON when stimulating the IC, range from 0.058 to 0.174, which can be considered to be representing weak cross-correlations between the area around the electrode and the other four specified ROIs. During the DBS-OFF periods these coefficients range from -0.013 to 0.093. There is only weak evidence supporting the alternative hypothesis that IC-stimulation results in a stronger cross-correlation found between the area around the electrode (encompassing the IC and parts of GP and RT) and the other specified ROIs during the DBS-ON periods compared to DBS-OFF. There is moderate evidence to support the null hypothesis in the cases of the cross-correlation coefficients found between the area around the electrode and the NAc, and the medial dorsal thalamus, giving moderate evidence to support the hypothesis that these cross-correlation coefficients do not differ between DBS-ON and DBS-OFF (electrode-NAc: BF_{01} = 4.364, error% < 0.005; electrode-medial dorsal thalamus: BF_{01} = 5.043, error% < 0.005).

The cross-correlation coefficients found during DBS-ON in the rostral IC-stimulated group, range from 0.054 to 0.268, and from -0.152 to 0.156 during DBS-OFF, which in both cases indicate weak cross-correlations between the area around the electrode and other specified ROIs. For the cross-correlation coefficients measured between the area around the electrode (encompassing the IC and parts of GP and RT) and the OFC, and the NAc, moderate evidence supporting the alternative hypothesis was found, supporting the hypothesis that stimulating the rostral IC results in a stronger cross-correlation during DBS-ON compared to DBS-OFF between the area around the electrode and the OFC (DBS-ON: M = 0.260, SE = 0.100; DBS-OFF: M = 0.001, SE = 0.067), and the area around the electrode and the NAc (DBS-ON: M = 0.150, SE = 0.106; DBS-OFF: M = -0.152, SE = 0.080), with the data around 3 to 5 times more likely to occur under the alternative hypothesis

Table 5
Results from the cross-correlation analyses in the IC stimulated group. Shown here are the average cross-correlation coefficients (mean ± SEM) calculated during DBS-ON and DBS-OFF, and the Bayes factors (BF_{10} and BF_{01}) resulting from the paired t-test framework comparing those averages, assuming the one-tailed alternative hypothesis that DBS-ON results in higher cross-correlations compared to DBS-OFF. The results are shown for the internal capsule (IC) as DBS target location (IC –all, $n = 17$) and the sub-locations within the IC (IC -rostral, $n = 8$; IC -caudal, $n = 7$). Note that the area around the electrode encompasses the IC as well as parts of the global pallidus and the reticular thalamic nucleus. For each target location, t-tests were performed on the cross-correlation coefficients found between the area around the electrode tip and the four other ROIs (electrode = area around the electrode tip; mPFC = medial prefrontal cortex; OFC = orbitofrontal cortex; NAc = nucleus accumbens; mdThal = medial dorsal thalamus). Bayes factors displayed in bold indicate moderate or greater evidence found.

Stimulation location	ROI	ON	OFF	BF_{10}	BF_{01}
IC -all $n = 17$	electrode - mPFC	0.174 ± 0.061	0.021 ± 0.057	2.136	0.468
	electrode - OFC	0.141 ± 0.067	−0.013 ± 0.059	1.865	0.536
	electrode - NAc	0.058 ± 0.065	0.072 ± 0.089	0.229	**4.364**
	electrode - mdThal	0.064 ± 0.055	0.093 ± 0.054	0.198	**5.043**
IC –rostral $n = 8$	electrode - mPFC	0.268 ± 0.104	0.083 ± 0.053	1.380	0.725
	electrode - OFC	0.260 ± 0.100	0.001 ± 0.067	**4.779**	0.209
	electrode - NAc	0.150 ± 0.106	−0.152 ± 0.080	**3.134**	0.319
	electrode - mdThal	0.054 ± 0.112	0.156 ± 0.049	0.225	**4.448**
IC -caudal $n = 7$	electrode - mPFC	0.116 ± 0.062	−0.071 ± 0.112	2.630	0.380
	electrode - OFC	0.061 ± 0.079	−0.057 ± 0.120	0.775	1.291
	electrode - NAc	0.013 ± 0.078	0.326 ± 0.132	0.163	6.144
	electrode - mdThal	0.041 ± 0.045	0.042 ± 0.108	0.351	2.847

than under the null hypothesis (electrode-OFC: $BF_{10} = 4.779$, error% < 0.0001; electrode-NAc: $BF_{10} = 3.134$, error% < 0.0001). The robustness checks for this Bayes factors show Bayes factor ranges of 4.0 to 4.8, and 2.5 to 3.2 respectively, over a wide range of prior widths. Moderate evidence supporting the null hypothesis was found looking at the cross-correlation coefficients measured between the area around the electrode and the medial dorsal thalamus, indicating that stimulating the rostral IC does not result in a stronger cross-correlation between the area around the electrode and the medial dorsal thalamus during DBS-ON compared to DBS-OFF (electrode-medial dorsal thalamus: $BF_{01} = 4.448$, error% < 0.001).

The cross-correlation coefficients found during DBS-ON and DBS-OFF in the caudal IC-stimulated group, range from 0.013 to 0.116, and from -0.071 to 0.326 respectively, which in both cases indicate weak cross-correlations between the area around the electrode (encompassing the IC and parts of GP and RT) and other specified ROIs. There was only weak evidence found to support the alternative hypothesis that targeting the caudal IC as stimulation location results in stronger cross-correlations between the area around the electrode and the other specified ROIs during DBS-ON compared to DBS-OFF. Evidence to support the null hypothesis that caudal IC-stimulation does not result in stronger cross-correlations was found for the cross-correlation between the area around the electrode and the NAc (electrode-NAc: $BF_{01} = 6.144$, error% < 0.001).

In conclusion, these analyses provide moderate support for a stimulation-induced increase in the cross correlation between the rostral IC area and the OFC and NAc.

4. Discussion

In this study, we compared how DBS in two target areas affects brain activity measured with BOLD fMRI in awake rats. The targets were the IC and the VMS, which are common loci for DBS therapy in treatment-refractory OCD. Our previous results showed that stimulation of both these areas strongly reduced compulsive self-grooming in transgenic mice (Pinhal et al., 2018). However, IC stimulation was more effective, while a different spectrum of behavorial effects was observed in both rats and mice (van Dijk et al., 2013; Pinhal et al., 2018). Here, we now report effects on brain activity that are both similar and differential, as well. IC stimulation resulted in a substantially higher activity measured around the tip of the electrodes, in particular in a subgroup with more caudally positioned electrodes. Moreover, stimulation of more rostral IC targets resulted in increased cross-correlations (i.e., connectivity) between activity in the IC area and the orbitofrontal cortex and the nucleus accumbens.

Stimulation of the more dorsal VMS (i.e., caudate) targets resulted in a strong increase in activity in the IC area, suggesting that increased activity in this area is a common result of both IC and VMS stimulations. VMS stimulation did not alter cross-correlations between the area of stimulation and any of the ROIs. Together, these results show that rodent fMRI is a promising approach to study the neural correlates of the anti-compulsive effects of DBS in animal models for OCD and to elucidate the mechanisms of its therapeutic effects in treatment-refractory OCD patients.

The IC and VMS targets used in this study were chosen because of their differential DBS effects on fear and anxiety in rats and genetically-induced compulsive grooming in Sapap3 mutant mice (van Dijk et al., 2013; Pinhal et al., 2018). Increases in pERK- or Fos-expression in stimulation sites and prefrontal areas of rats and mice suggested that fibers connecting these areas with the DBS targets were stimulated (Rodriguez-Romaguera et al., 2012; Pinhal et al., 2018). Stimulation of fiber tracts running through the human ventral anterior IC or the nucleus accumbens has proven clinical effectiveness in patients suffering from OCD (Denys et al., 2020; Tyagi et al., 2019; Senova et al., 2019; Liebrand et al., 2019; Li et al., 2020). Imaging studies in these patients revealed that stimulation eventually results in altered (in most studies: decreased) activity in prefrontal and striatal areas and in normalization of excessive corticostriatal connectivity (van Westen et al., 2015; Karas et al., 2018). Therefore, we focused on the question of whether DBS in rats could also alter activity and connectivity in the cortex-basal ganglia-thalamus circuits. Our results suggest that this is the case and that the effects of IC and VMS stimulation were partly overlapping.

We present two main findings which are both not only novel but also remarkable, because of the involvement of the IC. While the IC is a clinical target, animal studies considering the role of the IC are sparse. The first finding is the increase in connectivity between rostral IC (stimulation site) and OFC and NAc. This result can be expected as the fibers stimulated in the rostral IC will at least partly originate in the orbitofrontal cortex and have passed through the accumbens part of the VMS. Using anesthetized rats, Albaugh et al. (2016) report many changes in connectivity during NAc stimulation. Although the IC area as we studied it was not included, a suppression in cross-correlation was observed between the NAc and the external globus pallidus, probably close to the IC. In OCD patients, excessive connectivity was reported to be normalized by DBS (van Westen et al., 2015; Karas et al., 2018). Therefore, the use of an awake rat model for OCD is needed to decide if DBS has similar effects on connectivity as in the clinics.

The second finding is that stimulation both in the IC and in the VMS leads to increased activity in the IC area. When we divided our VMS group in a dorsal cohort (targeting the ventromedial caudate) and a ventral cohort (targeting the accumbens), it was the dorsal group which showed the strong increase in activity in the IC area. This may be another indication that DBS impacts the corticofugal fibers running from medial and orbital prefrontal areas through the medial striatum, into the

anterior IC, where they follow a path in the IC that is increasingly more ventral (Coleman et al., 1997; Kita and Kita, 2012; Coizet et al., 2017). It is tempting to conclude that stimulation of both VMS and IC may act on the same set of corticofugal fibers leading to increased activity in the IC area – the difference being that at the more rostral position the fibers are more spread out, whereas more caudally the fibers are densely packed in the IC. This is similar to what has recently been proposed for the human DBS targets in OCD, where stimulation of the same bundle of fibers at different rostral-caudal positions leads to similar therapeutic effects (Li et al., 2020; Smith et al., 2021).

The fact that we see BOLD activation of the IC area after stimulation in both targets is intriguing and requires further interpretation. One explanation for our findings might be the limited resolution of the BOLD images. Where voxels encompass multiple tissue objects, partial volume artifacts and spillover may occur, leading to impaired spatial resolution and erroneous signal intensities. Hence, the observed activation in the IC area might stem from artifacts caused by different tissue types bordering the IC in the same acquisition voxel. A second possibility is the heterogeneity of the IC area, including nearby other tissues such as GP and RT. The GP, in particular, has been implicated in brain circuits involved in the effects of DBS of OCD (Baldermann et al., 2021), was an effective DBS target to decrease compulsivity in a rat model (Klavir et al., 2011), and in fact has been used as a clinical target for OCD, for Tourette syndrome and for dystonia (Nair et al., 2014; Johnson et al., 2021; Vidailhet et al., 2013). Finally, the IC proper may show to be activated using various techniques, even though it is commonly thought that white matter areas such as the IC do not show significant BOLD activation and do not show activation when other techniques are used. There is, however, growing evidence suggesting that increased signal transduction resulting in increased BOLD or glucose metabolism is possible in white matter (Gawryluk et al., 2014; Sharp et al., 1983; Smith et al., 2019). On a microscopic level, increases in e.g. stimulation-induced expression of c-Fos have often been shown in white matter glia (Zhang et al., 1992; Tian and Bishop, 2002; Dragunow and Faull, 1989 Cancel et al., 2022). Moreover, the presence of neurons (as possible activity-mediating elements in white matter structures) has repeatedly been reported (Berezhnaya 2005; Suárez-Solá et al., 2009; DeFelipe et al., 2010). In line with this, we previously reported increased Fos-expression in the direct vicinity of DBS electrodes in the IC, i.e. the same area showing increased BOLD activity in our present results (Pinhal et al., 2018). The fact that increased Fos was restricted to the direct vicinity of the electrodes (see also Derksen et al., 2021), suggests that involvement of neighboring areas is less probable. Combined, these data provide support for the possibility that the white matter IC area does show increased BOLD activity and that activation of this area might be a possible key region in the IC- and VMS-mediated DBS effects. Future studies are needed to decide whether apparent activation of the IC is explained by one of the three above mentioned mechanisms.

Our study is the first in which the effects of DBS on BOLD activity was determined in awake rats. Studies in awake rats have been described before (King et al., 2005; Febo, 2011; Liang et al., 2013) and we have outlined the advantages of using awake animals in a previous study in which we tested and validated our set-up (Derksen et al., 2021). If we compare our results with those of previous studies in anesthetized rats, the number of areas in which altered activation or connectivity were observed was rather limited, whereas Albaugh et al. (2016), stimulating the nucleus accumbens, report activation in almost all areas that are known to be connected to this area, with increases or decreases in functional connectivity between many of these areas. The low number of alterations that we see may seem counterintuitive – as anesthesia generally dampens brain activity and decreases neurovascular coupling one would expect stronger activations and more widespread effects of DBS in awake animals. A tentative explanation may be that the awake state comes with more physiological variability in brain activity and with more noise due to movement artefacts or stress. This would then lead to a higher threshold for the detection of activations, so that the less interesting effects are filtered out and the more relevant changes are highlighted. The use of anesthesia was, however, not the only difference between the study of Albaugh et al. (2016) and ours – their use of CBV with contrast agent and a higher magnetic field strength may explain part of the difference as well.

There are some limitations to our study. The most important of these is the use of normal animals. This hampers a close comparison with the clinical studies referred to. Future studies will need to incorporate the use of one of the many behavioral or pharmacological rat models for OCD (Albelda and Joel, 2012; Szechtman et al., 2017). A further limitation is the relatively low resolution of our MRI methods. This may be the reason why we have not been able to confirm previous findings of prefrontal activation after IC or VMS stimulation (Pinhal et al., 2018; Rodriguez-Romaguera et al., 2012). The use of more sensitive fMRI techniques such as CBV with contrast agents (Albaugh et al., 2016) did also result in prefrontal activity after NAc DBS and might be applied in our MRI set-up, as well. On the other hand, the use of awake animals in fMRI studies of DBS is novel and an important advantage.

Our conclusion is that BOLD fMRI studies using a clinical scanner in awake rats are able to detect the changes in brain activity and connectivity induced by DBS of the IC or the VMS. Our results provide a first possible insight in the common and different effects of DBS in the two targets areas, VMS and IC. Further studies informed by our present results should elucidate both the (similar) anticompulsive effects common to these targets and the differences, thereby providing important information on the mechanisms of DBS in treatment-refractory OCD.

Data availability statement

All data described in this manuscript was gathered solely by the authors and is available upon request through the corresponding author. Prior to availability a data sharing agreement and agreement on co-authorship, depending on the extend of the use of the data, will be discussed and drafted.

Declaration of Competing Interest

None of the authors have any conflicts of interest associated with this study.

References

Albaugh, D.L., Salzwedel, A., Van Den Berge, N., Gao, W., Stuber, G.D., Shih, 2016. Functional magnetic resonance imaging of electrical and optogenetic deep brain stimulation at the rat nucleus accumbens. Sci. Rep. 6, 31613. https://doi.org/10.1038/srep31613.

Albelda, N., Joel, D, 2012. Current animal models of obsessive compulsive disorder: an update. Neuroscience 211, 83–106. https://doi.org/10.1016/j.neuroscience.2011.08.070.

Baldermann, J.C., Schüller, T., Kohl, S., Voon, V., Li, N., Hollunder, B., Figee, M., Haber, S.N., Sheth, S.A., Mosley, P.E., Huys, D., Johnson, K.A., Butson, C., Ackermans, L., Bouwens van der Vlis, T., Leentjens, A.F.G., Barbe, M., Visser-Vandewalle, V., Kuhn, J., Horn, A., 2021. Connectomic deep brain stimulation for obsessive-compulsive disorder. Biol. Psychiatry 90 (10), 678–688. https://doi.org/10.1016/j.biopsych.2021.07.010. Nov 15Epub 2021 Jul 19. PMID: 34482949.

Berezhnaya, L.A., 2005. NADPH-diaphorase-positive cells in the thalamic nuclei and internal capsule in humans. Neurosci. Behav. Physiol. 35 (3), 273–279. MarPMID: 15875489.

Cancel, L.M., Silas, D., Bikson, M., Tarbell, J.M., 2022. Direct current stimulation modulates gene expression in isolated astrocytes with implications for glia-mediated plasticity. Sci. Rep. 12 (1), 17964. https://doi.org/10.1038/s41598-022-22394-8. Oct 26PMID: 36289296; PMCID: PMC9606293.

Coizet, V., Heilbronner, S.R., Carcenac, C., et al., 2017. Organization of the anterior limb of the internal capsule in the rat. J. Neurosci. 37 (10), 2539–2554. https://doi.org/10.1523/JNEUROSCI.3304-16.2017.

Coleman, K.A., Baker, G.E., Mitrofanis, J., 1997. Topography of fibre organisation in the corticofugal pathways of rats. J. Comp. Neurol. 381 (2), 143–157. https://doi.org/10.1002/(sici)1096-9861(19970505)381:2<143::aid−cne3>3.0.co;2-3.

Defelipe, J., Fields, R.D., Hof, P.R., Höistad, M., Kostovic, I., Meyer, G., Rockland, K.S., 2010. Cortical white matter: beyond the pale remarks, main conclusions and discussion. Front. Neuroanat. 4, 4. https://doi.org/10.3389/neuro.05.004.2010. Mar 24PMID: 20428509; PMCID: PMC2859874.

Denys, D., Graat, I., Mocking, R., de Koning, P., Vulink, N., Figee, M., Ooms, P., Mantione, M., van den Munckhof, P., Schuurman, R., 2020. Efficacy of deep brain stimulation of the ventral anterior limb of the internal capsule for refractory obsessive-compulsive disorder: a clinical cohort of 70 patients. Am. J. Psychiatry 177 (3), 265–271. https://doi.org/10.1176/appi.ajp.2019.19060656. Mar 1Epub 2020 Jan 7. PMID: 31906709.

Derksen, M., Rhemrev, V., van der Veer, M., Jolink, L., Zuidinga, B., Mulder, T., Reneman, L., Nederveen, A., Feenstra, M., Willuhn, I., Denys, D., 2021. Animal studies in clinical MRI scanners: a custom setup for combined fMRI and deep-brain stimulation in awake rats. J. Neurosci. Methods 360, 109240. https://doi.org/10.1016/j.jneumeth.2021.109240. Aug 1Epub 2021 Jun 5. PMID: 34097929.

Dragunow, M., Faull, R.L., 1989. Rolipram induces c-fos protein-like immunoreactivity in ependymal and glial-like cells in adult rat brain. Brain Res. 501 (2), 382–388. https://doi.org/10.1016/0006-8993(89)90655-0. Nov 6PMID: 2510905.

Febo M. Technical and conceptual considerations for performing and interpreting functional MRI studies in awake rats. Front. Psychiatry. 2011 Jul 12;2:43. doi: 10.3389/fpsyt.2011.00043. PMID: 21808625; PMCID: PMC3137945.

Gawryluk, J.R., Mazerolle, E.L., D'Arcy, R.C, 2014. Does functional MRI detect activation in white matter? A review of emerging evidence, issues, and future directions. Front. Neurosci. 8, 239. https://doi.org/10.3389/fnins.2014.00239. Aug 8PMID: 25152709; PMCID: PMC4125856.

Graat, I., Mocking, R., Figee, M., Vulink, N., de Koning, P., Ooms, P., Mantione, M., van den Munckhof, P., Schuurman, R., Denys, D., 2021. Long-term outcome of deep brain stimulation of the ventral part of the anterior limb of the internal capsule in a cohort of 50 patients with treatment-refractory obsessive-compulsive disorder. Biol. Psychiatry 90 (10), 714–720. https://doi.org/10.1016/j.biopsych.2020.08.018. Nov 15Epub 2020 Aug 28. PMID: 33131717.

Haber, S.N., Yendiki, A., Jbabdi, S., 2021. Four deep brain stimulation targets for obsessive-compulsive disorder: are they different? Biol. Psychiatry 90 (10), 667–677. https://doi.org/10.1016/j.biopsych.2020.06.031. Nov 15Epub 2020 Jul 25. PMID: 32951818.

Hageman, S.B., van Rooijen, G., Bergfeld, I.O., Schirmbeck, F., de Koning, P., Schuurman, P.R., Denys, D., 2021. Deep brain stimulation versus ablative surgery for treatment-refractory obsessive-compulsive disorder: a meta- analysis. Acta Psychiatr. Scand. 143 (4), 307–318. https://doi.org/10.1111/acps.13276. AprEpub 2021 Feb 11. PMID: 33492682.

Jeffreys, H., 1961. Theory of Probability, 3rd edn. Oxford Univeristy Press, Oxford.

Johnson, K.A., Duffley, G., Foltynie, T., et al., 2021. Basal Ganglia pathways associated with therapeutic pallidal deep brain stimulation for Tourette syndrome. Biol. Psychiatry Cogn. Neurosci. Neuroimaging 6 (10), 961–972. https://doi.org/10.1016/j.bpsc.2020.11.005.

Karas, P.J., Lee, S., Jimenez-Shahed, J., Goodman, W.K., Viswanathan, A., Sheth, S.A., 2019. Deep brain stimulation for obsessive compulsive disorder: evolution of surgical stimulation target parallels changing model of dysfunctional brain circuits. Front. Neurosci. 12, 998. https://doi.org/10.3389/fnins.2018.00998. Jan 8PMID: 30670945; PMCID: PMC6331476.

King, J.A., Garelick, T.S., Brevard, M.E., Chen, W., Messenger, T.L., Duong, T.Q., Ferris, C.F., 2005. Procedure for minimizing stress for fMRI studies in conscious rats. J Neurosci Methods 148 (2), 154–160. https://doi.org/10.1016/j.jneumeth.2005.04.011. Oct 30Epub 2005 Jun 16. PMID: 15964078; PMCID: PMC2962951.

Kita, T., Kita, H., 2012. The subthalamic nucleus is one of multiple innervation sites for long-range corticofugal axons: a single-axon tracing study in the rat. J. Neurosci. 32 (17), 5990–5999. https://doi.org/10.1523/JNEUROSCI.5717-11.2012.

Klanker, M., Feenstra, M., Willuhn, I., Denys, D., 2017. Deep brain stimulation of the medial forebrain bundle elevates striatal dopamine concentration without affecting spontaneous or reward-induced phasic release. Neuroscience 364, 82–92. https://doi.org/10.1016/j.neuroscience.2017.09.012.

Klavir, O., Winter, C., Joel, D, 2011. High but not low frequency stimulation of both the globus pallidus and the entopeduncular nucleus reduces 'compulsive' lever-pressing in rats. Behav. Brain Res. 216 (1), 84–93. https://doi.org/10.1016/j.bbr.2010.07.018.

Li, N., Baldermann, J.C., Kibleur, A., Treu, S., Akram, H., Elias, G.J.B., Boutet, A., Lozano, A.M., Al-Fatly, B., Strange, B., Barcia, J.A., Zrinzo, L., Joyce, E., Chabardes, S., Visser-Vandewalle, V., Polosan, M., Kuhn, J., Kühn, A.A., Horn, A, 2020. A unified connectomic target for deep brain stimulation in obsessive-compulsive disorder. Nat. Commun. 11 (1), 3364. https://doi.org/10.1038/s41467-020-16734-3. Jul 3PMID: 32620886; PMCID: PMC7335093.

Liang, Z., Li, T., King, J., Zhang, N., 2013. Mapping thalamocortical networks in rat brain using resting-state functional connectivity. Neuroimage 83, 237–244. https://doi.org/10.1016/j.neuroimage.2013.06.029. DecEpub 2013 Jun 15. PMID: 23777756; PMCID: PMC3815960.

Liebrand, L.C., Caan, M.W.A., Schuurman, P.R., van den Munckhof, P., Figee, M., Denys, D., van Wingen, G.A, 2019. Individual white matter bundle trajectories are associated with deep brain stimulation response in obsessive-compulsive disorder. Brain Stimul. 12 (2), 353–360. https://doi.org/10.1016/j.brs.2018.11.014. Mar-AprEpub 2018 Nov 27. PMID: 30522916.

Nair, G., Evans, A., Bear, R.E., Velakoulis, D., Bittar, R.G., 2014. The anteromedial GPi as a new target for deep brain stimulation in obsessive compulsive disorder. J. Clin. Neurosci. 21 (5), 815–821. https://doi.org/10.1016/j.jocn.2013.10.003.

Paxinos, G., Watson, C., 2007. The Rat Brain in Stereotaxic Coordinates, 6th edn. Elsevier Press, Oxford.

Pinhal, C.M., van den Boom, B.J.G., Santana-Kragelund, F., Fellinger, L., Bech, P., Hamelink, R., Feng, G., Willuhn, I., Feenstra, M.G.P., Denys, D, 2018. Differential effects of deep brain stimulation of the internal capsule and the striatum on excessive grooming in sapap3 mutant mice. Biol. Psychiatry 84 (12), 917–925. https://doi.org/10.1016/j.biopsych.2018.05.011. Dec 15Epub 2018 May 23. PMID: 29954580.

Rodriguez-Romaguera, J., Do Monte, F.H., Quirk, G.J, 2012. Deep brain stimulation of the ventral striatum enhances extinction of conditioned fear. Proc. Natl Acad. Sci. U S A. 109 (22), 8764–8769. https://doi.org/10.1073/pnas.1200782109. May 29.

Senova, S., Clair, A.H., Palfi, S., Yelnik, J., Domenech, P., Mallet, L., 2019. Deep brain stimulation for refractory obsessive-compulsive disorder: towards an individualized approach. Front. Psychiatry 10, 905. https://doi.org/10.3389/fpsyt.2019.00905. Dec 13PMID: 31920754; PMCID: PMC6923766.

Sharp, F.R., Bzorgchami, S., Kilduff, T., 1983. Focal increases of white matter glucose utilization produced by stimulation of rat motor cortex. J. Cereb. Blood Flow Metab. 3 (1), 67–70. https://doi.org/10.1038/jcbfm.1983.8. PMID: 6822620.electrical. Mar.

Smith, H.R., Beveridge, T.J.R., Nader, S.H., Nader, M.A., Porrino, L.J., 2019. Regional elevations in microglial activation and cerebral glucose utilization in frontal white matter tracts of rhesus monkeys following prolonged cocaine self-administration. Brain Struct. Funct. 224 (4), 1417–1428. https://doi.org/10.1007/s00429-019-01846-4. MayEpub 2019 Feb 12. PMID: 30747315; PMCID: PMC6510647.

Suárez-Solá M.L., González-Delgado F.J., Pueyo-Morlans M., Medina-Bolívar O.C., Hernández-Acosta N.C., González-Gómez M., Meyer G. Neurons in the white matter of the adult human neocortex. Front. Neuroanat. 2009 Jun 9;3:7. doi: 10.3389/neuro.05.007.2009. PMID: 19543540; PMCID: PMC2697018.

Smith, A.H., Choi, K.S., Waters, A.C., Aloysi, A., Mayberg, H.S., Kopell, B.H., Figee, M., 2021. Replicable effects of deep brain stimulation for obsessive-compulsive disorder. Brain Stimul. 14 (1), 1–3. https://doi.org/10.1016/j.brs.2020.10.016. Oct 28Epub ahead of print. PMID: 33130018.

Szechtman, H., Ahmari, S.E., Beninger, R.J., et al., 2017. Obsessive-compulsive disorder: insights from animal models. Neurosci. Biobehav. Rev. 76, 254–279. https://doi.org/10.1016/j.neubiorev.2016.04.019. Pt B.

Tian, J.B., Bishop, G.A., 2002. Stimulus-dependent activation of c-Fos in neurons and glia in the rat cerebellum. J. Chem. Neuroanat. 23 (3), 157–170. https://doi.org/10.1016/s0891-0618(01)00153-3. MarPMID: 11861123.

Tyagi, H., Apergis-Schoute, A.M., Akram, H., Foltynie, T., Limousin, P., Drummond, L. M., Fineberg, N.A., Matthews, K., Jahanshahi, M., Robbins, T.W., Sahakian, B.J., Zrinzo, L., Hariz, M., Joyce, E.M., 2019. A randomized trial directly comparing ventral capsule and anteromedial subthalamic nucleus stimulation in obsessive-compulsive disorder: clinical and imaging evidence for dissociable effects. Biol. Psychiatry 85 (9), 726–734. https://doi.org/10.1016/j.biopsych.2019.01.017. May 1Epub 2019 Jan 30. PMID: 30853111; PMCID: PMC6467837.

van Dijk, A., Klanker, M., van Oorschot, N., et al., 2013. Deep brain stimulation affects conditioned and unconditioned anxiety in different brain areas. Transl. Psychiatry 3 (7), e289. https://doi.org/10.1038/tp.2013.56. Published 2013 Jul 30.

van Westen, M., Rietveld, E., Figee, M., Denys, D, 2015. Clinical outcome and mechanisms of deep brain stimulation for obsessive-compulsive disorder. Curr. Behav. Neurosci. Rep. 2 (2), 41–48. https://doi.org/10.1007/s40473-015-0036-3. PMID: 26317062; PMCID: PMC4544542.

van Westen, M., Rietveld, E., Bergfeld, I.O., et al., 2021. Optimizing deep brain stimulation parameters in obsessive-compulsive disorder. Neuromodulation 24 (2), 307–315. https://doi.org/10.1111/ner.13243.

van Doorn, J., van den Bergh, D., Böhm, U., Dablander, F., Derks, K., Draws, T., Wagemakers, E.-J., 2021. The JASP guidelines for conducting and reporting a Bayesian analysis. Psychon. Bull. Rev. 28, 813–826. https://doi.org/10.3758/s13423-020-01798-5.

Vidailhet, M., Jutras, M.F., Grabli, D., Roze, E, 2013. Deep brain stimulation for dystonia. J. Neurol. Neurosurg. Psychiatry 84 (9), 1029–1042. https://doi.org/10.1136/jnnp-2011-301714.

Zhang, P., Hirsch, E.C., Damier, P., Duyckaerts, C., 1992. Javoy-Agid F. c-fos protein-like immunoreactivity: distribution in the human brain and over-expression in the hippocampus of patients with Alzheimer's disease. Neuroscience 46 (1), 9–21. https://doi.org/10.1016/0306-4522(92)90004-l. PMID: 1594107.